AIAA 80-1383R

Characterization of the Auroral Ionosphere Using Optical Remote-Sensing Techniques

R. D. Sears*
Lockheed Palo Alto Research Laboratories, Palo Alto, Calif.

This paper reviews the theoretical and technological basis for determining some of the properties of the auroral ionosphere by optical remote-sensing techniques. Spectrophotometer and imaging experiments are described which provide detailed, quantitative information on properties of the *E* region: total energy deposited, ion pair production rate, electron density, and height-integrated Hall and Pederson conductivities. Examples of these measurements are given and compared with equivalent measurements made using the Chatanika incoherent scatter radar. It is shown that measurements made with spectrophotometric methods compare well in accuracy with the radar measurements.

Introduction

A GENERAL understanding of the morphology of the aurora and of the magnetospheric processes leading to these impressive displays has been derived from visual and photographic observations made over the last half century. However, detailed descriptions of the nature of the precipitating particle fluxes and their effects upon the ionosphere have been approached only during the last decade or so with the advent of in-situ rocket and satellite-borne probes as well as sophisticated spectrophotometric remote-sensing optical instrumentation.

This presentation reviews the theoretical and technological basis for application of optical remote-sensing techniques to a description of the auroral processes which deposit energy at high latitudes in the Earth's atmosphere. The use of these techniques to determine the response of the ionosphere to the auroral particle flux is described.

Analytical Basis for Visible Near-Infrared Spectrophotometry

Extensive quantitative spectrophotometric measurements of the intensities, morphology, and occurrence statistics of many auroral emission features have been made. These are summarized in several review articles.[1,2] However, quantitative understanding of the parameters of the principal precipitating particle fluxes (electrons and protons) can be obtained by careful photometric observations of only a few spectroscopic emission features, namely, the H_α or H_β emissions at 656.3 and 486.1 nm, respectively, the forbidden emissions of OI at 557.7 and 630.0 nm, and one or more of the first negative bands of N_2^+ (e.g., 0-0 band at 391.4 nm or 0-1 band at 427.8 nm).

Several workers have developed analytical relationships between the incoming fluxes of protons and electrons and observed spectrophotometric features of the above-mentioned emissions.[3,4] The work presented in this article centers on the theoretical model developed by Rees and Luckey,[4] which allows the total energy deposit by electrons to be determined from the 427.8 nm N_2^+ first negative band intensity and which allows the mean energy parameter of an assumed Maxwellian energy distribution for the precipitating electron flux to be determined from the ratios $R_1 = I(630.0\ \text{nm})/I(427.8\ \text{nm})$ and $R_2 = I(557.7\ \text{nm})/I(427.8\ \text{nm})$ which are derived from spectrophotometric measurements. A simplified representation of the Rees and Luckey model is illustrated in Fig. 1.

Instrumentation

Recent technological advances which have been made in narrowband spectral filter construction, digital photon-counting electronics, and sensitive image-intensified TV detectors have been incorporated into the spectrophotometric and imaging detectors described in this section. Coupling of high-responsivity extended spectral range photomultipliers to digital photon counting and recording electronics allows very high sensitivity, high spectral resolution spectrophotometry to be accomplished. A typical digital photon-counting, multispectral photometer is illustrated in Fig. 2.[5] This instrument is a direct descendant (although highly improved) of the photometers fielded during the International Geophysical Year[6] and further developed by Eather and Mende.[7] An example of multispectral photometric data obtained during a pulsating aurora is given in Fig. 3.

Development of multistage image-intensifier tubes during the recent decade has allowed even very weak spectral emissions from the upper atmosphere to be imaged and presented in a TV display format. Hence, combination of these intensified detectors with narrowband spectral filters and sophisticated computer-based control logic allows one to view and to analyze the subvisual emissions from the upper atmosphere in terms of the physical and chemical processes which are related to specific emission features. A block diagram of a typical image-intensified auroral all-sky TV system is presented in Fig. 4.[8] Images derived from this system in two spectral regions, the 427.8 nm 1 NG (first negative) band of N_2^+ and the 630.0 nm emission line of O, are illustrated in Fig. 5. Digitized representations of such images can be used to determine the auroral particle flux characteristics as well as the response of the ionosphere as described in the following sections.

Optical Characterization of the Auroral Precipitating Flux

The principal energetic charged particles which create the visible aurora and consequently enhance the ionospheric electron density are protons and electrons. The spatial and temporal morphology of these particle fluxes can be mapped using either spectrophotometric instruments which are operated in a scanning mode or by use of the IITV system

Presented as Paper 80-1383 at the 13th Annual AIAA Fluid and Plasma Dynamics Conference, Snowmass, Colo., July 14-17, 1980; submitted Dec. 3, 1980; revision received July 8, 1981.

*Staff Scientist.

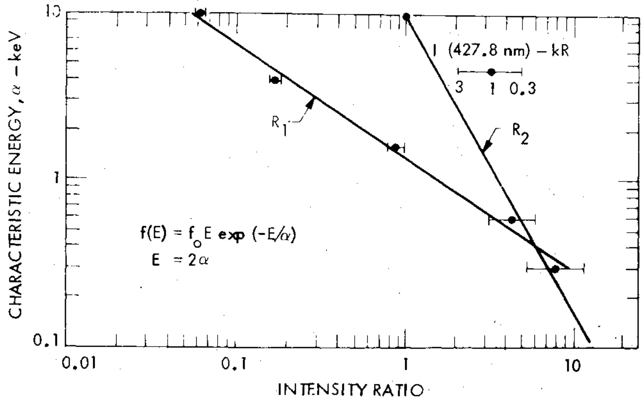

Fig. 1 Theoretical model which relates the characteristic energy parameter of an energetic precipitating auroral electron flux to the observed spectrophotometric ratios R and R_2. This model is a simplification of that produced by Rees and Luckey.[4]

which gives a series of snapshots of the auroral morphology as illustrated, for example, in Fig. 5. Both photometric and imaging instrumentation can be calibrated with sufficient precision that the theoretical techniques described in a previous section can be applied in order to determine the total energy and mean energy parameters of the precipitating electron flux.

A variety of techniques have been developed to optimize the presentation of the intensity data in terms of spatial, temporal, or spectral morphology. Examples of the temporal morphology of auroral precipitating electron energy flux, plus the characteristic energy parameter, are provided in Figs. 6 and 7. Figure 6 is in the format of a KEOGRAM,[9] in which the latitudinal variation of the relevant parameters is plotted as a function of time. The absolute values of the quantities presented are indicated by the density of the gray scale. A more conventional plot of the same quantities is illustrated in Fig. 7.[10] In both cases illustrated here, the photometers were scanned in the magnetic meridian such that an ionospheric swath approximately 800 km in extent was covered.

Response of the Ionosphere to Auroral Precipitation

Auroral precipitation creates excess ionization in all regions of the ionosphere depending upon the total energy of the precipitating flux, its characteristic energy (or penetrating power), and relative balance between electron and proton constituents. Auroral ionization and its effects upon radio wave propagation have been monitored and described by numerous workers over the last several decades. However, only recently has it been possible to describe the response of the ionosphere by spectrophotometric techniques. These techniques depend upon the specification of a multiparameter model for the precipitating electron (and proton) flux by means of spectrophotometric measurements described in previous sections. In this section, we show how the auroral E region can be modeled from spectrophotometric data over a range of auroral conditions.

Construction of an electron density model for conditions of auroral precipitation requires a model for the effective recombination coefficient as a function of altitude and some means of defining the temporal stationarity of the precipitating electron flux. For most conditions of auroral precipitation, it is reasonable to assume that a quasiequilibrium condition exists in the ionosphere such that the following condition holds: $dN_e/dt = Q - \alpha_{eff} N_e^2 = 0$. Transport has been ignored in this formulation. Examination of direct electron density measurements, ionization source temporal variations, and the recombination coefficient value as a function of altitude for many auroral conditions indicates that this approximation is adequate at least for the E region.[11]

Numerous theoretical and numerical methods have been used to determine the altitude distribution of the ionizing source function Q, given either a detailed numerical or a parametric description of the precipitating electron flux above the atmosphere. Fortunately, it has been found that the altitude distribution of Q in the E region is not very sensitive to the detailed physical parameters of the flux, such as the pitch angle distribution, and details of the energy distribution.[11] The total energy flux and the characteristic energy parameter for a pseudo-Maxwellian energy distribution have been applied to several codes (Auroral,[12] Rees, and SRI TANGLE[13]) to determine Q as a function of altitude. Except for a few problems relating to low-energy electrons (<1 keV), all of these computation techniques produce substantially the same value of Q vs altitude. Given Q and α_{eff} (from Ref. 14), computation of the value of N_e vs altitude is straightforward. An example of the computation of N_e as a function of altitude for an intense aurora is illustrated in Fig. 8. This figure also shows a direct comparison between the electron density profile derived from spectrophotometric measurements and the TANGLE code and that measured using the Chatanika incoherent scatter radar.

Given that spectrophotometric measurements can provide a useful and reliable model of ionospheric electron density in

Fig. 2 Block diagram of a digitally controlled, photon-counting spectrophotometer. The system illustrated as well as similar systems are commonly interfaced to minicomputer and/or microprocessor computer control systems.

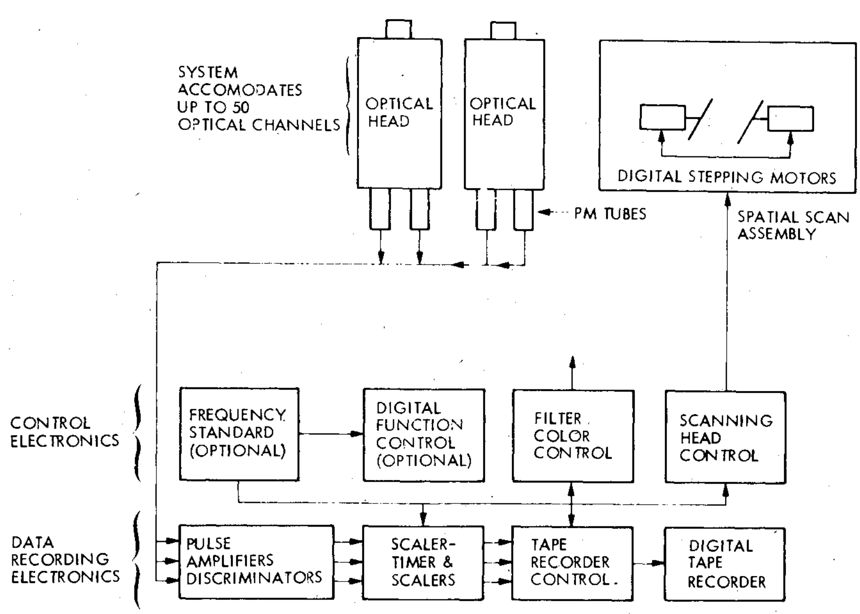

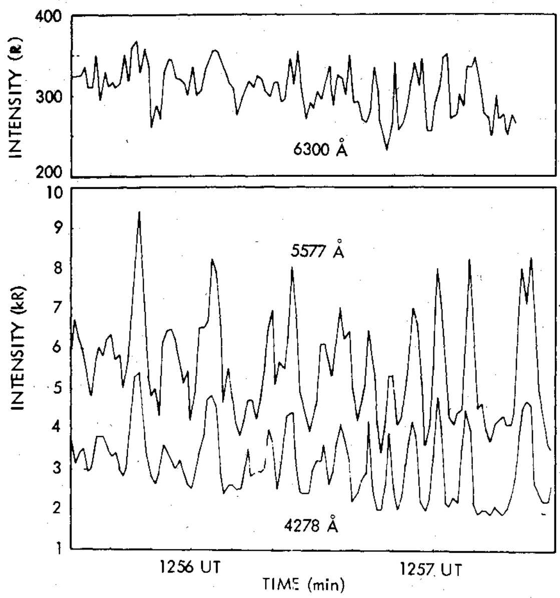

Fig. 3 Spectrophotometric data taken by a photon-counting photometer system during a pulsating aurora. Three spectral channels are illustrated. Data were obtained on nine spectral channels simultaneously with a temporal resolution of 1 s.

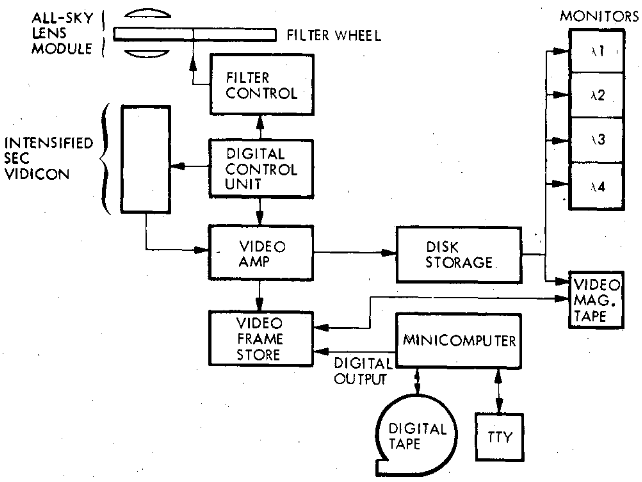

Fig. 4 Block diagram of a multispectral image-intensified TV (IITV) imaging system. This system may be controlled by a minicomputer or a microprocessor, and monitors and displays images in four successive wavelength channels. Optical coverage is over 150 deg of the sky.

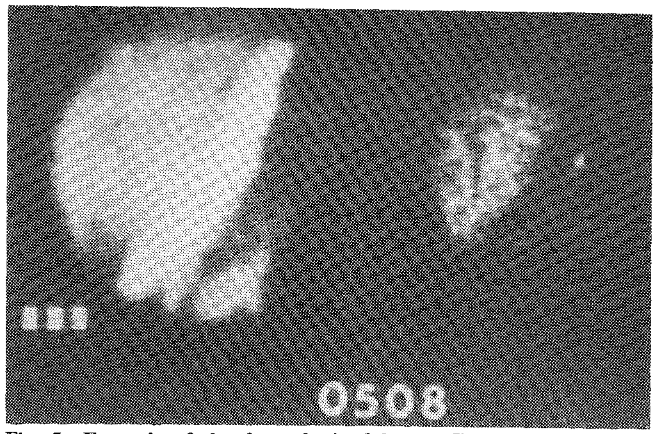

Fig. 5 Example of the data obtained by the IITV system in two wavelength regions. Each picture represents a 150 deg all-sky view of the optical emissions. The left picture is representative of emission caused by relatively low-energy auroral particles as contrasted to the right-hand picture which characterizes the overall energy deposited by the aurora in the atmosphere.

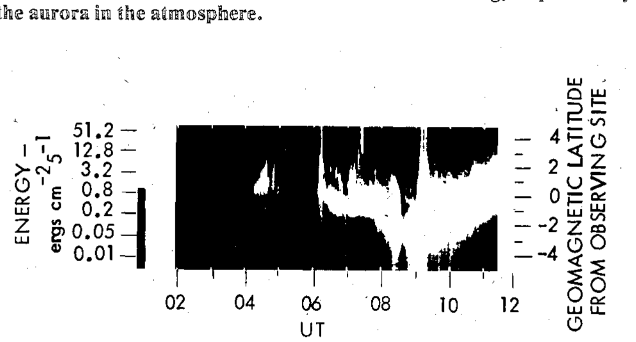

Fig. 6 Plot of the distribution of auroral emission vs latitude and time derived from meridional scanning photometer data. The form of the plot is a KEOGRAM wherein the intensity of the energy deposit is characterized by the gray scale intensity. Note: 1 deg of geomagnetic latitude approximates 110 km, so that the KEOGRAM represents auroral intensity variations over about 900 km range in latitude.

the E region during auroral activity, one may then apply a model for ionic Hall and Pederson mobilities and derive the height-integrated Hall and Pederson conductivities. These quantities are especially important for derivation of the electric current patterns associated with auroral conditions. Up to the present time, these quantities have been derived mainly through the use of incoherent scatter radar measurements. Figure 9 illustrates comparisons of conductivity results obtained during coordinated radar-photometer measurements.[15] As can be seen, the height-integrated Pederson conductivities obtained from the two independent techniques compare well; in contrast, there appears to be a systematic underestimation of Hall conductivity from the photometer technique as compared with the radar technique. The source of this moderate systematic disagreement at large values of Hall conductivity is not determined at present.

Verification of Spectrophotometric Measurements

Ground- and aircraft-based spectrophotometric intensity and imaging measurements have been shown to provide useful information relevant to the auroral precipitation morphology as well as the response of the auroral E region. It is desirable, however, to verify independently the accuracy of the quantities derived or inferred from spectrophotometric measurements. For example, numerous comparisons of rocket-based precipitating particle measurements[16] with ground-based photometric measurements of auroral spectral features have been conducted. A consensus of the published data appears to indicate that careful ground-based photometric measurements provide accurate characterization of the precipitating electron and proton flux, to within the error limits of the technique (typically a 10-30% combined statistical and systematic error).

Spectrophotometric measurement techniques and the IITV measurements presented herein depend to a significant degree upon the care taken in defining and quantitatively specifying a number of important experimental parameters: instrument spectrophotometric calibration, atmospheric extinction vs wavelength, and the zenith angle effects caused by varying extinction and the Van Rijn effect. Most of the data presented herein are based upon more extensive studies reported in the appropriate references which dealt with these factors.

Atmospheric extinction, for example, is based upon a clear arctic atmosphere model, which is then degraded depending upon visual observations of stars of known magnitude. Because the measurements reported herein were made in central Alaska, at Chatanika, we were able to assume on a reasonable basis that the atmosphere was stable enough within our nominal scan range ±80 deg zenith angle that tropospheric scatter was constant under our good to excellent seeing conditions. Comparison of the atmospheric extinction vs the Van Rijn effect shows that they are self-compensatory

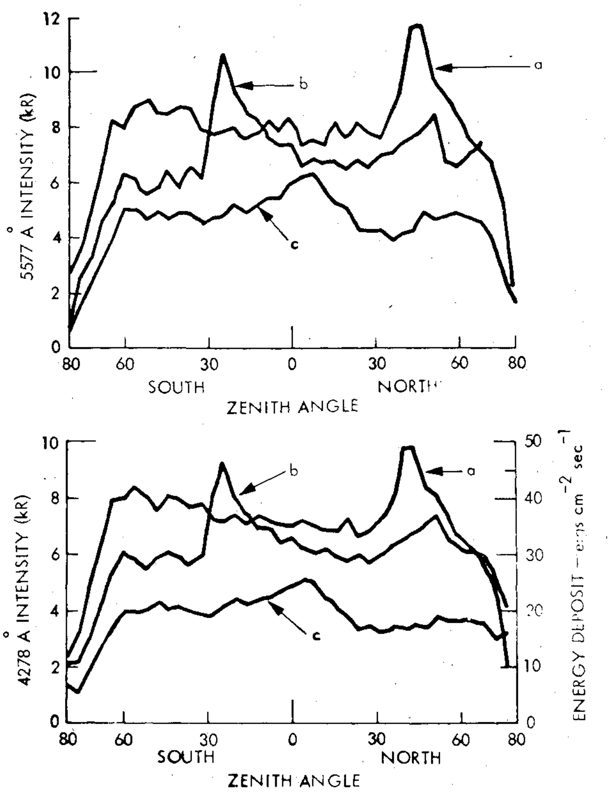

Fig. 7 Conventional plot of auroral spectral intensities obtained during three successive scans of a multispectral, photon-counting photometer. Digitized data obtained in this format may be conveniently converted into the KEOGRAM format by offline processing.

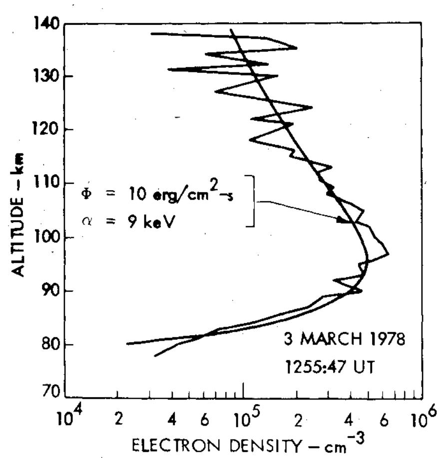

Fig. 8 Comparison of electron density vs altitude curve modeled from spectrophotometer data with incoherent scatter radar measurements made at the same time. Both optical and radar fields of view were boresighted such that the ionospheric volume observed was nearly identical. Measurements were made at Chatanika, Alaska.

within a given zenith angle, depending upon the extinction coefficients. In practice, these effects compensate one another, within experimental error (20%), to a zenith angle of about 50-60 deg in a clear arctic atmosphere.

Calibration of the IITV system is more complex. Internal calibration using an internal radioactive light source is conducted, but with sometimes varying accuracy because of temperature hysteresis of the phosphor emitter, and because of the low-emission intensity. The internal calibration source is augmented by meridional scanning spectrophotometric data which are used finally to calibrate the IITV data frames after digitization. A fairly complex computer-based routine is used for this procedure. Results of the application of the cross-calibration procedure sampled from a data base of over 200 frames of IITV data are described by Kumer et al.[17]

An intensive effort has been conducted to verify ionospheric properties which are inferred from spectrophotometric data with other independent measurements. This effort has centered about simultaneous spectrophotometric intensity measurements and incoherent scatter radar measurements using the Chatanika, Alaska, incoherent scatter radar and optical instrumentation located at this site. Previous sections have referred to comparative measurements of E region electron density profiles, and height-integrated Hall and Pederson conductivities.

The author and collaborators have found good agreement between radar and photometer-derived quantities. In most cases, total energy deposit, characteristic energy parameter, electron density profile data, and height-integrated Pederson conductivity data agree well within mutual experimental errors (30%). Poorer agreement has been found for height-integrated Hall conductivities, but this discrepancy may lie more within the conductivity models used than with the basic measurements.

Summary and Conclusions

This paper has described advances in spectrophotometric and image-intensified TV characterization of the auroral region particle precipitation and the response of the ionosphere to the energetic particles. Optical remote-sensing techniques have their own obvious limitations, but also have been shown to provide a useful supplement to radio frequency measurements of the auroral ionosphere. These conclusions are reinforced by efforts described here which show that accurate characterization of auroral particle energy deposit, characteristic energy parameter, ionospheric electron density profile, and height-integrated Hall and Pederson conductivities can be obtained from spectrophotometric data. The accuracy of spectrophotometrically derived quantities has been verified by comparison with other observing techniques.

Acknowledgments

The author wishes to thank his colleagues at LMSC and at SRI International for contributions which were necessary to the compilation of a review paper of this type. Special contributions were made by Dr. S. B. Mende of LMSC, Dr. R. R.

Fig. 9 Comparison of height-integrated Hall and Pederson conductivities derived from optical spectrophotometric data and from incoherent scatter radar models. Both instruments scanned in the magnetic meridian, i.e., along the same horizontal swath through the ionosphere. Measurements were made at Chatanika, Alaska.

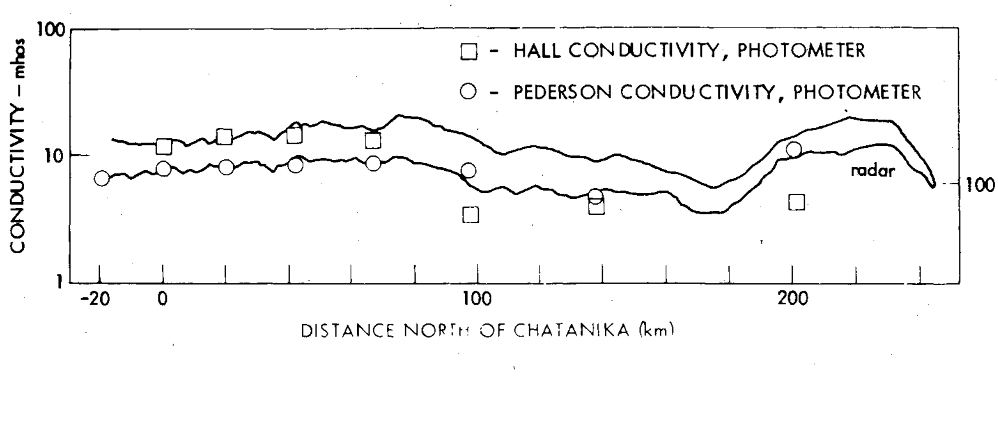

Vondrak of SRI International, and the operating crew of Chatanika Incoherent Scatter Radar facility, which is operated by SRI International. This publication was written under the support of the LMSC Independent Research Program. Optical and incoherent scatter radar measurements cited in this report were supported under various contracts from Defense Nuclear Agency and from the National Science Foundation as referenced in the appropriate articles.

References

[1] Chamberlain, J. W., *Physics of the Aurora and Airglow*, Academic Press, New York, 1961.

[2] Jones, A. V., *Aurora*, D. Reidel Publishing Co., Dordrecht, the Netherlands, 1976.

[3] Kamayama, H., "The Dependence of the Relative Intensity of Some of the Auroral Lines upon the Energy Spectrum of Precipitating Electrons," *Science Reports of the Tohoku University*, Vol. 18, 1967, p. 8390.

[4] Rees, M. H. and Luckey, D., "Auroral Electron Energy Derived from Ratio of Spectroscopic Emissions: 1, Model Computations," *Journal of Geophysical Research*, Vol. 79, Dec. 1974, pp. 5181-5186.

[5] Sears, R. D., "Versatile Family of Modular Aurora and Airglow Photometers," *Applied Optics*, Vol. 12, June 1973, p. 1349.

[6] Eather, R. H. and Reasoner, D. L., "Spectrophotometry of Faint Light Sources with a Tilting-Filter Photometer," *Applied Optics*, Vol. 8, Feb. 1969, p. 227.

[7] Mende, S. B. and Eather, R. H., "Spectroscopic Determination of the Characteristics of Precipitating Auroral Particles," *Journal of Geophysical Research*, Vol. 80, Aug. 1975, pp. 3211-3216.

[8] Mende, S. B., Eather, R. H., and Aamodt, E. K., "All-Sky Monochromatic Imaging at Very Low Light Levels," *Applied Optics*, Vol. 16, June 1977, pp.1691-1700.

[9] Mende, S. B. and Eather, R. H., "Monochromatic All-Sky Observations and Auroral Precipitation Patterns," *Journal of Geophysical Research*, Vol. 81, Aug. 1976, pp. 3771-3780.

[10] Davidson, G. T. and Sears, R. D., "Pulsating Aurorae; Evidence for Flux Limiting," *Geophysical Research Letter*, No. 7, March 1980, pp. 185-188.

[11] Vondrak, R. R. and Sears, R. D., "Comparison of Incoherent Scatter Radar and Photometric Measurements of the Energy Distribution of Auroral Electrons," *Journal of Geophysical Research*, Vol. 83, April 1978, pp. 1665-1667.

[12] Banks, P. M., Chappell, C. R., and Nagy, A. F., "A New Model for the Interaction of Auroral Electrons with the Atmosphere; Spectral Degradation, Backscatter, Optical Emissions and Ionization," *Journal of Geophysical Research*, Vol. 79, April 1974, pp. 1459-1470.

[13] Vondrak, R. R. and Baron, M. J., "A Method of Obtaining the Energy Distribution of Auroral Electrons from Incoherent Scatter Radar Measurements," *Radar Probing of the Auroral Plasma*, Scandinavian University Books, Oslo, Norway, 1977, pp. 315-330.

[14] Wickwar, V. B., Baron, M. J., and Sears, R. D., "Auroral Energy Input from Energetic Electrons and Joule Heating at Chatanika," *Journal of Geophysical Research*, Vol. 80, Nov. 1975, pp. 4364-4367.

[15] Sears, R. D. and Vondrak, R. R., "Latitudinal Distribution of Ionospheric Conductivity in the Auroral Region," *EOS, Transactions of AGU*, Vol. 58, 1977, p. 1206.

[16] Baker, K. D., "Coordinated Rocket Measurements of Auroral Parameters," *Annales de Geophysique*, Vol. 24, 1968, pp. 285-289.

[17] Kumer, J. B., Sears, R. D., Evans, J. E., Harris, S. E., and Nadile, R. M., "Application of Visible Monochromatic Auroral Imaging Data for Modeling Infrared Earthlimb Morphology," AIAA Paper 81-0423, Jan. 1981.